

Probing Behavior of *Dichelops furcatus* (F.) (Heteroptera: Pentatomidae) on Wheat Plants Characterized by Electropenetrography (EPG) and Histological Studies

Tiago Lucini¹ and Antônio Ricardo Panizzi^{2,3}

¹Department of Zoology, Federal University of Paraná, P.O. Box 19020, Curitiba, PR 81531-980 Brazil, (tiago_lucini@hotmail.com; antonio.panizzi@embrapa.br), ²Laboratory of Entomology, Embrapa National Wheat Research Center, P.O. Box 3081, Passo Fundo, RS 99001-970, Brazil, and ³Corresponding author, e-mail: antonio.panizzi@embrapa.br

Subject Editor: Phyllis Weintraub

Received 17 January 2017; Editorial decision 9 April 2017

Abstract

The stink bug *Dichelops furcatus* (F.) (Heteroptera: Pentatomidae) has increased in abundance in recent years on the wheat, *Triticum aestivum* L., crop cultivated in the southern region of Brazil. To investigate the probing (stylet penetration) behaviors and nonprobing behaviors of *D. furcatus* on wheat plants, the electrical penetration graph or electropenetrography (EPG) technique was applied. Nine EPG waveforms (types/subtypes) were identified and described on stem and on ear head of wheat plants, as follows: Z, Np, Df1a, Df1b, Df2, Df3a, Df3b, Df4a, and Df4b. For the waveforms Df1, Df2, Df3, and Df4, stylets were severed to determine, via histological studies, the location of the stylet tip and/or salivary sheath tip in plant tissue. Waveform Z was visually correlated with the bug standing still on the plant surface, whereas during Np the bug was walking. Df1a and Df1b represent initial stylet insertion, deep penetration of the stylets into the plant tissue, and secretion of salivary sheath. Df2 represents xylem sap ingestion on stem and on ear head. Waveforms Df3a and Df4a were related to the cell rupturing feeding strategy (laceration and maceration tactics) on stem and on ear head (seed endosperm), respectively. Waveforms Df3b and Df4b represent ingestion of cellular contents derived from cell rupturing activities on stem and on ear head (seed endosperm), respectively. With this fundamental knowledge in hand, future studies can use EPG to develop novel pest management solutions.

Key words: electronic feeding monitoring, feeding, histology, *Triticum aestivum* L, waveform identification

The Neotropical stink bug *Dichelops furcatus* (F.), commonly called green-belly stink bug, occurs in different countries of South America; in Brazil, it is recorded more often in the southern region (Chiaradia et al. 2011). This stink bug is reported to feed on several plant species, including cultivated and non-cultivated plants (Smaniotto and Panizzi 2015). Among the cultivated plants, *D. furcatus* has been observed as a pest of soybean, *Glycine max* (L.) Merrill, since the 1970s (Panizzi et al. 1977).

More recently, *D. furcatus* was observed to feed on heads of sunflower, *Helianthus annuus* L. (Frota and Santos 2007), and on seedlings of corn, *Zea mays* (L.) causing injury that ended in seed yield loss (Roza-Gomes et al. 2011). Damage on this latter plant is similar to that of the congener *Dichelops melacanthus* (Dallas) (Ávila and Panizzi 1995, Chocorosqui and Panizzi 2004), which also feeds on the reproductive structures of host plants. On wheat plants, *Triticum aestivum* L., *D. furcatus* damages the crop in Southern Brazil causing seed yield reduction (Chocorosqui and Panizzi 2004, Panizzi et al. 2016), where it has been observed to increase in abundance. Another pentatomid, *Thyanta perditor* (F.), has also been

observed to cause damage on wheat plants cultivated in Brazil (Ferreira and Silveira 1991). In the United States (from Georgia north to Minnesota), several other pentatomids species are reported on wheat, mainly species of the genus *Euschistus* [*Euschistus servus* (Say), *Euschistus variolarius* (Palisot de Beavois), and *Euschistus ictericus* (L.)], and *Oebalus pugnax* (F.) (Buntin and Greene 2004, Koch et al. 2016).

D. furcatus feeds on both vegetative and reproductive stages, causing significant damage to cultivated plants (Panizzi et al. 2016). Because of its recent occurrence in wheat fields and because of lack of information on its feeding behavior, more studies are needed to better understand its feeding on wheat plants in different phenological stages. To do so, the technique known as electrical penetration graph (EPG) or electropenetrography is useful; in this technique, any piercing-sucking insect and a plant are made part of a simple electrical circuit where a low current flows through a circuit, composed of plant and feeding insect.

Both probing and nonprobing activities are captured by the EPG system and are presented as waveforms on computer screen

(Tjallingii 1978, Walker 2000). For pentatomids, despite their economic importance, only three species have had their feeding behavior characterized using EPG [*Edessa mediatubunda* (F.), and *Piezodorus guildinii* (Westwood) on soybean plants (Lucini and Panizzi 2016 and Lucini et al. 2016, respectively) and *D. melacanthus* on maize seedlings (Lucini and Panizzi 2017)]. This is the fourth study applying EPG technology to stink bugs, in this case, *D. furcatus* on wheat plants. It should yield valuable information on its feeding on an economic host plant with potential to be used on its chemical control targeting the action of systemic insecticides.

The objectives of this study were, therefore, to 1) create a waveform library characterizing the EPG waveforms produced by *D. furcatus* feeding on wheat plants during vegetative (stem) and reproductive (ear head) stages, 2) determine the biological meanings of each waveform recorded via electrical characteristics and histological studies; and 3) determine the feeding sites exploited by the bug on the vegetative and reproductive plant stages.

Materials and Methods

Stink Bugs and Wheat Plants

Adults of *D. furcatus* were field-collected at the Embrapa Wheat Research Center during May to July 2016 located in Passo Fundo, RS, Brazil (28° 15' S, 52° 24' W). Stink bugs were weekly collected on wheat plants, taken to the laboratory and placed into rearing cages (25 × 20 × 20 cm), lined with filter paper to develop colonies. The cages were kept in a walk-in chamber at 25 ± 1 °C, 65 ± 10% RH, and a photoperiod of 14:10 (L:D) h.

A standard food source was provided for the stink bugs, composed of a mixture of green bean pods, *Phaseolus vulgaris* L., raw shelled peanuts, *Arachis hypogaea* L., mature seeds of soybean, *Glycine max* (L.) Merrill, and wheat seedlings; the mixture was replaced once per week. During this time, eggs were collected and placed inside of small plastic boxes (11 × 11 × 3.5 cm) to raise nymphs to obtain adults to be used in the experiments.

Wheat seeds cv. BRS Parrudo (Embrapa) were seeded weekly in small (100 ml) and big (2 liters) pots kept in the greenhouse. Plants in stage 3 (V3: tillering stage) grown in small pots and plants in stage 11.1 (R11.1: milk grain stage) (Large 1954) grown in big pots were separated and used in EPG recordings during vegetative and reproductive stages, respectively. Plants were grown using a standard oxy-soil prepared for greenhouse studies at Embrapa.

EPG Recordings and Analysis of the Waveforms

The feeding behavior of *D. furcatus* on wheat plants was monitored using a four-channel alternating current (AC)-direct current (DC) monitor (Backus and Bennett 2009; EPG Technologies, Inc., Gainesville, FL). Before starting EPG recordings, adult-females (of approximately 2-wk old originated from eggs laid by field-collected adults) were removed from the laboratory colony, placed in a small plastic box (11 × 11 × 3.5 cm) lined with filter paper and starved for ca. 15 h before wiring. Then, the stink bugs were wired according to the methodology described by Lucini and Panizzi (2016). This methodology consists in sanding the cuticle of the pronotum of bugs to improve the wire attachment.

After this procedure, stink bugs were individually connected to an EPG amplifier and placed on stem wheat during vegetative stage and on ear head during reproductive stage. To close the electrical circuit, the copper plant electrode (3-cm long) was inserted into the soil of a pot containing each plant. Insects, plants, and the four

head-stage amplifiers (channels) were kept inside a Faraday cage. At the vegetative stage, the wheat seedlings were kept with their stems vertically positioned, whereas at the reproductive stage, the wheat plants containing a selected ear head were laid down along a plastic support (11 × 11 cm) and held in place using strips of Parafilm (Pechiney Plastic Packaging, Menasha, WI). The plastic support was held horizontally by an alligator clip connected to a “helping hand” holder.

Waveforms caused by changes in electrical origins, i.e., Resistance and electromotive force (emf) components, were captured and digitized at a sample rate of 100 Hz per channel using a DI-710 (Dataq Instruments, Akron, OH) and recorded by using a HP Pentium notebook with WinDaq Lite software (Dataq). Offset and gain settings were adjusted for optimum view of the waveforms and to avoid rectifier fold-over to retain native waveform polarity after rectification (Backus and Bennett 2009). To characterize the waveforms, we considered the following characteristics: shape, frequency, amplitude, and electrical origin (R and emf components). The frequency and amplitude were manually calculated by expanding the x-axis to minimum compression and counting (see details of the methodology by Lucini and Panizzi 2016). In addition, we used histological techniques to correlate the waveforms and feeding sites, as done previously with three other species of pentatomids (Lucini and Panizzi 2016, 2017; Lucini et al. 2016).

Experimental Design

In the EPG experiment, we applied two different input impedance (Ri) levels, 10⁷ and 10⁹ Ohms, and a standardized voltage level of 50 mV of AC. Eighty insects were successfully recorded, i.e., 40 stink bugs per Ri level (20 during vegetative stage and 20 during reproductive stage at each Ri level). The stink bugs were monitored undisturbed for an 8-h access period, in a closed room with controlled conditions (25 ± 2 °C) and continuous light. Representative waveforms excerpts at each Ri level were assembled using Microsoft Power Point (Microsoft Corporation, Redmond, WA).

Histological Analysis to Determine the Stylet and/or Salivary Sheath Position in Plant Tissue

Plant histology was conducted to determine the position of stylet and/or salivary sheath tip of *D. furcatus* on stem and on ear head, which allowed us to correlate each feeding site with the different waveforms observed during EPG AC-DC recordings. For that, a set of *D. furcatus* adult-females were recorded at Ri 10⁷ Ohms and 50 mV AC signal. The EPG monitor was turned off every time a specific waveform was observed, and then the stylets were carefully cut using an entomological micro-scissors. After that, the plant tissues containing severed stylets were processed to prepare semi-permanent slides according to Lucini and Panizzi (2016).

For the stem histology, we used wheat plants in stage 8 (–8 - flag leaf visible) (Large 1954), because the stem is more rigid allowing clean cuts of plant tissue (the feeding behavior and waveforms recorded in younger and older plants stages were the same). The position of the stylet tips and/or salivary sheath tips in stem and in ear head structures were determined based on 10 samples for waveform Df1a, 12 for Df2, 11 for Df3a, and 10 for Df4a. Digital images were captured using Olympus BX50 (Shinjuku, Tokyo, Japan) microscope coupled with a Sony DXC 107A video camera (Minato, Tokyo, Japan) linked to a computer.

Results

General Overview of *Dichelops furcatus* Waveforms on Wheat Plants

The waveform coarse structure recorded for *D. furcatus* on wheat plants on vegetative and reproductive stages included nine different waveforms, which represented non-probing and probing activities. Regarding the nomenclature, probing waveform types were denoted as Df [from *Dichelops furcatus*] plus a number and subtypes by an additional, lower-case letter, as used for other pentatomids (Lucini and Panizzi 2016, 2017; Lucini et al. 2016).

Two of those waveforms recorded represent nonprobing behavior, namely, Z and Np, whereas probing waveforms were represented by another four waveforms, namely, Df1, Df2, Df3, and Df4. All these waveforms, except Df2, were sub-divided into two different subtypes each, as follows: Df1a and Df1b, Df3a and Df3b, and Df4a and Df4b. The probing waveforms were grouped in two different families: pathway (P) and ingestion (I). The family P consisted of two waveforms (Df1a and Df1b), and family I consisted of five waveforms (Df2, Df3a, Df3b, Df4a, and Df4b). In both plant structures evaluated (stem and ear head), waveforms presented similar characteristics (electrical and appearance); therefore, all waveforms were grouped in the same table (Table 1).

Nonprobing Waveforms. Represented by two waveforms, Z and Np (Fig. 1A), nonprobing waveforms that were visually correlated with their biological meanings. Waveform Z occurred when the bug was standing still on the plant surface and was characterized by a very low amplitude without variation in appearance between Ri levels applied. Therefore, Z wave represented the baseline. Np was observed when the bug was walking on the plant surface; it was characterized by irregular peaks with variable amplitude according to Ri level applied. Results suggested a strong emf-component to Np wave although R was also present (Table 1).

Probing Waveforms. Two main waveform families (P and I) were described during feeding behavior of *D. furcatus* on stem and on ear head of wheat plants, and they comprised seven different types/subtypes, namely, Df1a, Df1b, Df2, Df3a, Df3b, Df4a, and Df4b. These will be described in the order in which they occurred during the feeding activities of *D. furcatus* on wheat plants. All probing waveforms, at both Ri levels (10^7 and $10^9\Omega$), occurred below 0 V (i.e., were monophasic negative).

Pathway Phase. Family P (Waveform Df1)

Df1 occurred after nonprobing waveforms, Z or Np, and it was divided in two subtypes: Df1a and Df1b. Df1a was recorded in both plant structures evaluated (stem and ear head); it was characterized by irregular-peaks without a clear pattern (Figs. 1B and E and 2A–C), and almost always presented the largest amplitude value in the probe among all the waveforms registered. The subtype Df1b was recorded only on wheat ear head, and it was characterized by a more distinct pattern (Fig. 2A–C) of random overlying/superimposed on low- to medium-amplitude waves (35 and 23% at Ri 10^7 and 10^9 Ohms, respectively), with a high and regular frequency, on average ranging from 4.7 to 5.1 Hz between Ri levels (Table 1). Df1b waveform always occurred after Df1a or alternating among events of Df1a (e.g., Df1a → Df1b → Df1a → Df1b, and so on) (Fig. 2B and C).

The subtype Df1b was not always present, and it was visually correlated with protraction and retraction movements of the stylets in the ear head tissue, especially when the bug inserted its stylets in the glume (outer layer) and in the lemma (layer below the glume that surrounds the seed). However, during recordings on stems to

make the histological sections, we also observed the presence of Df1b, because stems used to make the cuts were more developed and rigid (V8 stage). In general, both Df1a and Df1b were more clearly distinguished at Ri 10^7 Ohms (low Ri level) than at 10^9 Ohms (high Ri level), thus supporting R as their primary electrical origin (Table 1).

Df1a always preceded the waveform Df2 (see Ingestion Phase) recorded on wheat stem (Figs. 1C and E and 2A) and was also often observed before the waveform Df3a (see Ingestion Phase) (Figs. 3B and 4B). Otherwise, on ear head, the waveforms Df2 and Df4a (see below) were preceded by Df1a or Df1b. On stem and on ear head, the waveforms Df1 (both subtypes) and Df2 were easily distinguished from each other during recordings, and also between Ri levels (Figs. 1E and 2A). However, Df1 (both subtypes), Df3a (on stem), and Df4a (on ear head) were occasionally not clearly distinguished from one another, mainly when recorded at Ri 10^9 Ohms (Fig. 4B) (see Df3 and Df4).

Ingestion Phase. Family I (Waveforms Df2, Df3, and Df4)

The family I comprised five different waveforms, labeled Df2, Df3a, Df3b, Df4a, and Df4b.

Waveform Df2. Df2 was always observed immediately after waveform Df1a on stem (Fig. 1E), and Df1a (most frequently) and Df1b on ear head (Fig. 2A) of wheat plants. The waveform Df2 was composed of repetitive wave portions interspersed with peaks, in general, downward oriented, which occurred at regular intervals over time (Figs. 1A, C, D, F and 2A and D), peaks and waves are defined in Fig. 1C).

At both Ri levels (10^7 and 10^9 Ohms) and also on both plant structures evaluated, the appearance of waveform Df2 and its peak orientation were similar, except the amplitudes varied according to Ri level applied. Peak amplitude value was lower when applied Ri 10^7 Ohms (28%) compared to Ri 10^9 Ohms (60%) (Table 1). Regarding frequency, Df2 showed a regular pattern with means of 3.1 Hz at both Ri levels. Thus, waveform Df2 presented a mixture of electrical components, with peaks originating from R-component, because they were clearly distinguished at Ri 10^7 Ohms, as well as emf-component, because peaks were still clearly distinguished and separated from wave portion at high Ri level (10^9 Ohms). Wave portions were more emphasized at Ri 10^9 Ohms; thus, waves were emf-dominated (compare Fig. 1C and F).

Waveform Df3. Waveform Df3 was divided into two subtypes, Df3a and Df3b (Figs. 3A–E and 4A–F), which were recorded only when *D. furcatus* fed on wheat stem. Df3a was often recorded after a short event of waveform Df1a (Figs. 3B and 4B); however, the separation between them sometimes was not clear. Df3a was characterized by a generally stereotypical pattern with peaks oriented both upward and downward at both Ri levels (Figs. 3C and 4C). Df3a showed a similar frequency at both Ri levels (means of 3.1 and 3.0 Hz at Ri 10^7 and 10^9 Ohms, respectively). Nevertheless, Df3a was greatly variable in appearance (primarily amplitude) not only across Ri levels, but also among individual bugs and even within the same recording. As Ri level increased, the amplitude value decreased (57% at Ri 10^7 Ohms and 31% at Ri 10^9 Ohms) (Table 1). Thus, Df3a was R-dominated.

Waveform Df3b was characterized as a regular wave of short event durations (in general, a few seconds) at both Ri levels, always occurring interspersed with Df3a, as follows: Df3a → Df3b → Df3a → Df3b → and so on (Figs. 3D and E and 4D–F). Df3b was not always clearly from Df3a within recordings, or it did not occur.

Table 1. Summary of EPG AC-DC waveforms, their main electrical characteristics, and suggested biological meanings for each waveform recorded during probing and nonprobing activities of *D. furcatus* on stem and on ear head of wheat plants

Phase	Family	Type or subtype	Plant structure observed	Amplitude (%)		Frequency (Hz)		Electrical origin	Suggested biological meaning
				Ri 10 ⁷	Ri 10 ⁹	Ri 10 ⁷	Ri 10 ⁹		
Nonprobing	-	Z	Stem/ear head	Flat	Flat	-	-	-	Standing still on the plant surface
Pathway	P	Np	Stem/ear head	Low-medium	Medium-high	Irregular	Irregular	Mostly emf/some R	Walking on the plant surface
		Df1a	Stem/ear head	100	100	Irregular	Irregular	Mostly R	Stylet penetration and salivary sheath secretion
Ingestion	I	Df1b	Ear head	35 (16–100)	23 (13–37)	5.1 (4.2–5.7)	4.7 (3.8–5.8)	Mostly R	Bug encountering a rigid cell layer requiring stylet protraction and retraction
		Df2	Stem/ear head	28 (11–53)	60 (29–100)	3.1 (2.6–3.9)	3.1 (2.4–4.2)	Mixed; peak = R/emf; wave = emf-dominated	Xylem sap ingestion
Salivation/ingestion	I	Df3a	Stem	57 (37–90)	31 (19–52)	3.1 (2.8–3.5)	3.0 (2.9–3.2)	Mostly R; emf is also present	Cell laceration, enzymatic maceration of stem tissues and probably ingestion
Ingestion	I	Df3b	Stem	15 (7–19)	19 (15–22)	3.9 (3.5–4.2)	4.1 (4.0–4.2)	Mostly emf-component	Short ingestion of macerated stem tissues
Salivation	I	Df4a	Ear head	51 (32–79)	35 (18–55)	Mostly irregular + burst regular peaks 3.5 Hz	Mostly irregular + burst regular peaks 3.8 Hz	Mostly R; emf is also present	Cell laceration, enzymatic maceration of seed endosperm
Ingestion	I	Df4b	Ear head	20 (9–34)	27 (11–65)	3.5 (2.7–4.7)	4.0 (3.0–5.1)	Mostly emf-component	Ingestion of macerated seed endosperm

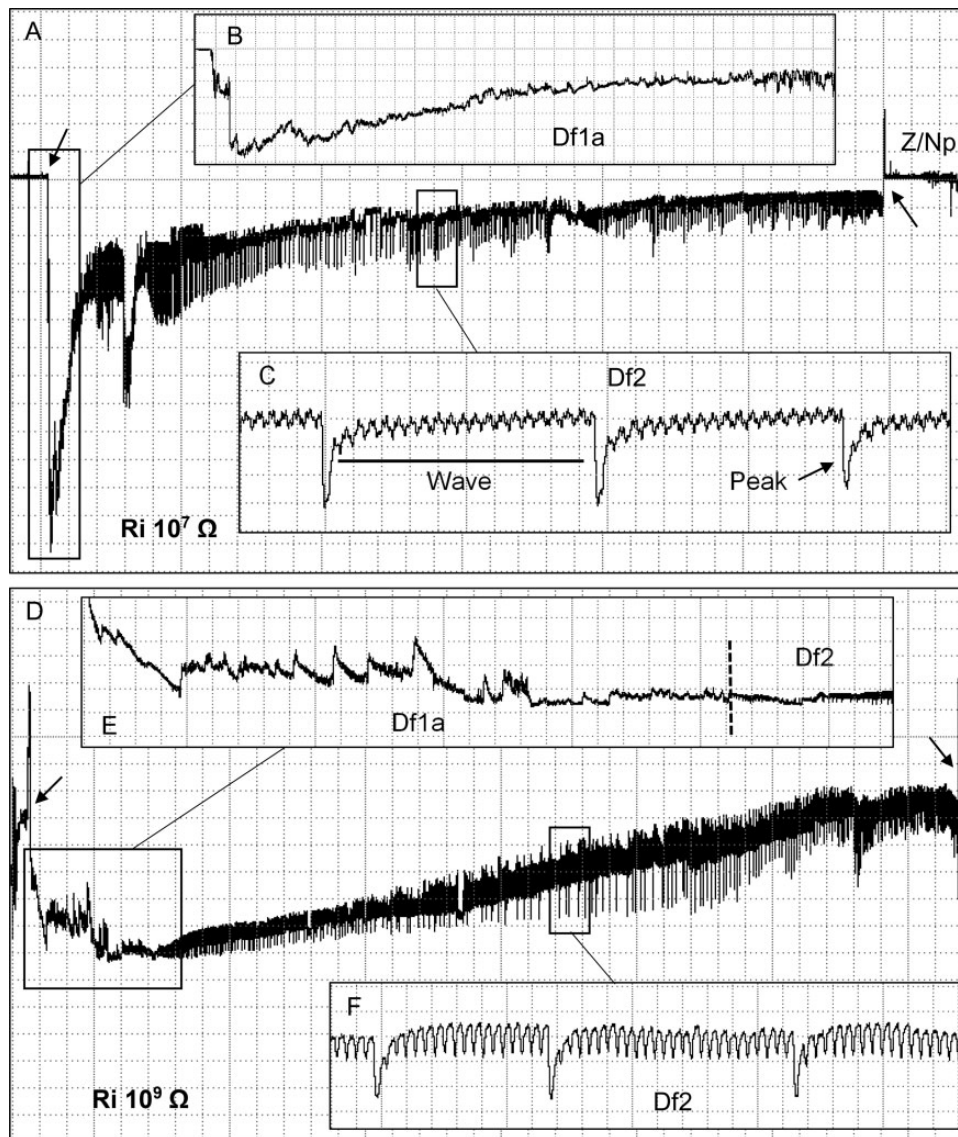


Fig. 1. Waveforms recorded using EPG AC-DC from *D. furcatus* on stems of wheat plants during vegetative stage (–3 – tillering stage) at Ri 10^7 Ohms (A–C) and Ri 10^9 Ohms (D–F). (A) Compressed overview of a probing event (~40 min), showing waveforms Df1a (pathway) and Df2 (xylem sap ingestion). (B) Expanded view of waveform Df1a. (C) Expanded view of waveform Df2 and definition of peak and wave portions. (D) Compressed overview of several waveform events (~35 min), showing Df1a and Df2. (E) Expanded view of waveform Df1a and beginning of waveform Df2. (F) Expanded view of waveform Df2. (A has Windaq compression 400 [80 s/vertical div.], gain 16 \times ; B has compression 25 [5 s/vertical div.], gain 8 \times ; C has compression 3 [0.6 s/vertical div.], gain 32 \times ; D has compression 300 [60 s/vertical div.], gain 8 \times ; E has compression 50 [10 s/vertical div.], gain 8 \times ; F has compression 5 [1 s/vertical div.], gain 8 \times). Arrowheads indicate beginning or end of a probe.

At both Ri levels, 10^7 and 10^9 Ohms, Df3b showed low-amplitude values (15 and 19%, respectively), as well as frequency values (3.9 and 4.1 Hz, respectively) (Table 1). Df3b, in the same way as Df3a, was quite variable across Ri levels, among different bugs and also within the same bug recording.

Regarding the electrical origin of the waveform Df3, it presented a mixture of electric components varying according to the wave subtype. Subtype Df3a, in general, showed a decrease in amplitude value when applied a Ri of 10^9 Ohms compared to a low Ri level (10^7 Ohms), indicating a R-component. However, this subtype was still clearly visible at 10^9 Ohms, indicating the emf-component, as well. Df3b was more emphasized at Ri 10^9 Ohms, thus emf is the main component (Table 1).

Waveform Df4. Waveform Df4 was also divided into two different subtypes, namely, Df4a and Df4b (Figs. 5A–D and 6A–D),

which were recorded only when *D. furcatus* fed on wheat ear head (seed endosperm). Df4a was, in general, preceded by a short Df1b wave, and sometimes by Df1a; however, in both cases, it was often hard to separate the waveforms Df1a/Df1b and Df4a within the recording, especially at Ri 10^9 Ohms (Fig. 6A). Df4a showed irregularity in appearance, different from Df2 and even Df3a (which latter represents the same feeding strategy of the Df4a wave, but performed in different tissues). Df4a presented a high-amplitude value when Ri of 10^7 Ohms was used (means of 51%) compared to 10^9 Ohms (35%). Therefore, Df4a originated mostly from R-component.

In addition, Df4a was characterized not only by overlying irregular frequency, composed of peaks negative and positive oriented at both Ri levels (Figs. 5A–C and 6A–C, Table 1) but also with underlying portions that were more regular (frequency

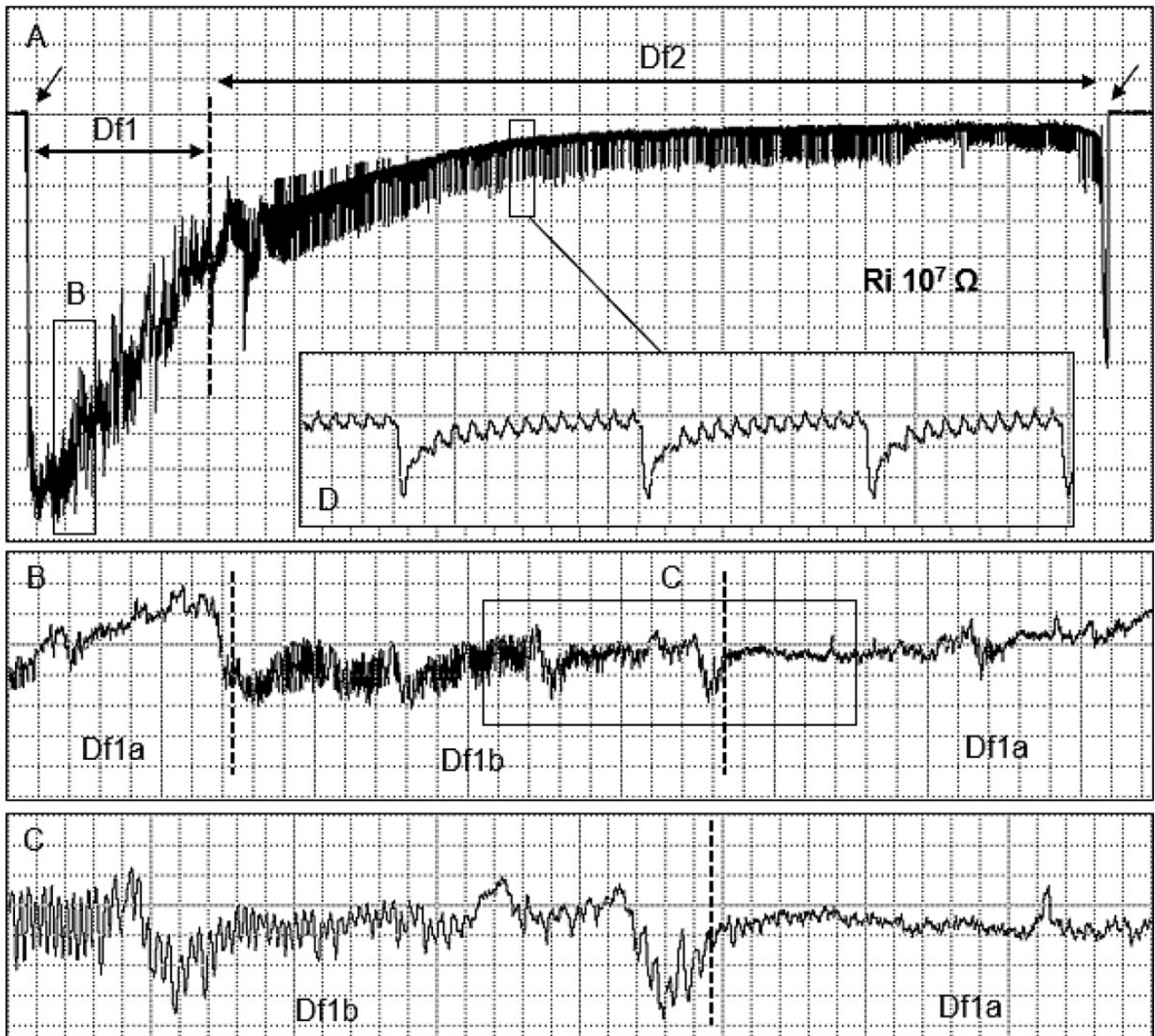


Fig. 2 Waveforms recorded using EPG AC-DC from *D. furcatus* on ear head of wheat plants during reproductive stage (R11.1: milk grain stage) at Ri 10^7 Ohms. (A) Compressed overview of several waveform events (~50 min), showing Df1 (pathway) and Df2 (xylem sap ingestion). (B) Expanded view of both Df1 subtypes, Df1a and Df1b. (C) Details of the waveforms Df1a and Df1b. (D) Expanded view of waveform Df2. (A has Windaq compression 400 [80 s/vertical div.], gain $8\times$; B has compression 10 [2 s/vertical div.], gain $8\times$; C has compression 3 [0.6 s/vertical div.], gain $16\times$; D has compression 3 [0.6 s/vertical div.], gain $16\times$). Arrowheads indicate beginning or end of a probe.

ranging from 3.5 to 3.8 Hz). Sometimes, within the same recording, peaks were positive and negative oriented, and this inversion was not due to rectifier fold-over (see Materials and Methods). Furthermore, Df4a was variable in appearance between Ri levels, but also among bugs and within the recording of the same insect. In contrast, Df4b showed a highly regular pattern of short event duration compared to Df4a, always occurring interspersed with the latter (Figs. 5C and Dand 6C and D). Df4b presented a mean amplitude value (20 and 27% at Ri 10^7 and 10^9 Ohms, respectively) and a regular frequency, ranging from 3.5 to 4.0 Hz between Ri levels (Table 1).

Df4 presented a mixture of electric components varying according to the wave subtype. Df4a showed a decrease in amplitude value when applied a Ri of 10^9 Ohms compared to a 10^7 Ohms, indicating a R-component. This subtype was still clearly

visible at 10^9 Ohms, indicating the emf-component, as well. Df4b was more emphasized at Ri 10^9 Ohms, thus emf is the main component (Table 1).

Correlations of the Waveforms and Their Specific Feeding Sites via Histological Analyses

Df1. In the waveform Df1a recorded during the feeding activities of *D. furcatus* on wheat plant, the presence of a salivary sheath surrounding the stylets was observed in all histological sections on stem ($n = 10$) (Fig. 7A). Furthermore, the tip of the salivary sheath and/or stylets terminated in cells of the parenchyma, confirming that Df1a represents pathway phase (insertion and penetration of the stylets deep into the plant tissue and secretion of the salivary sheath). However, there was an interesting difference about secretion of the

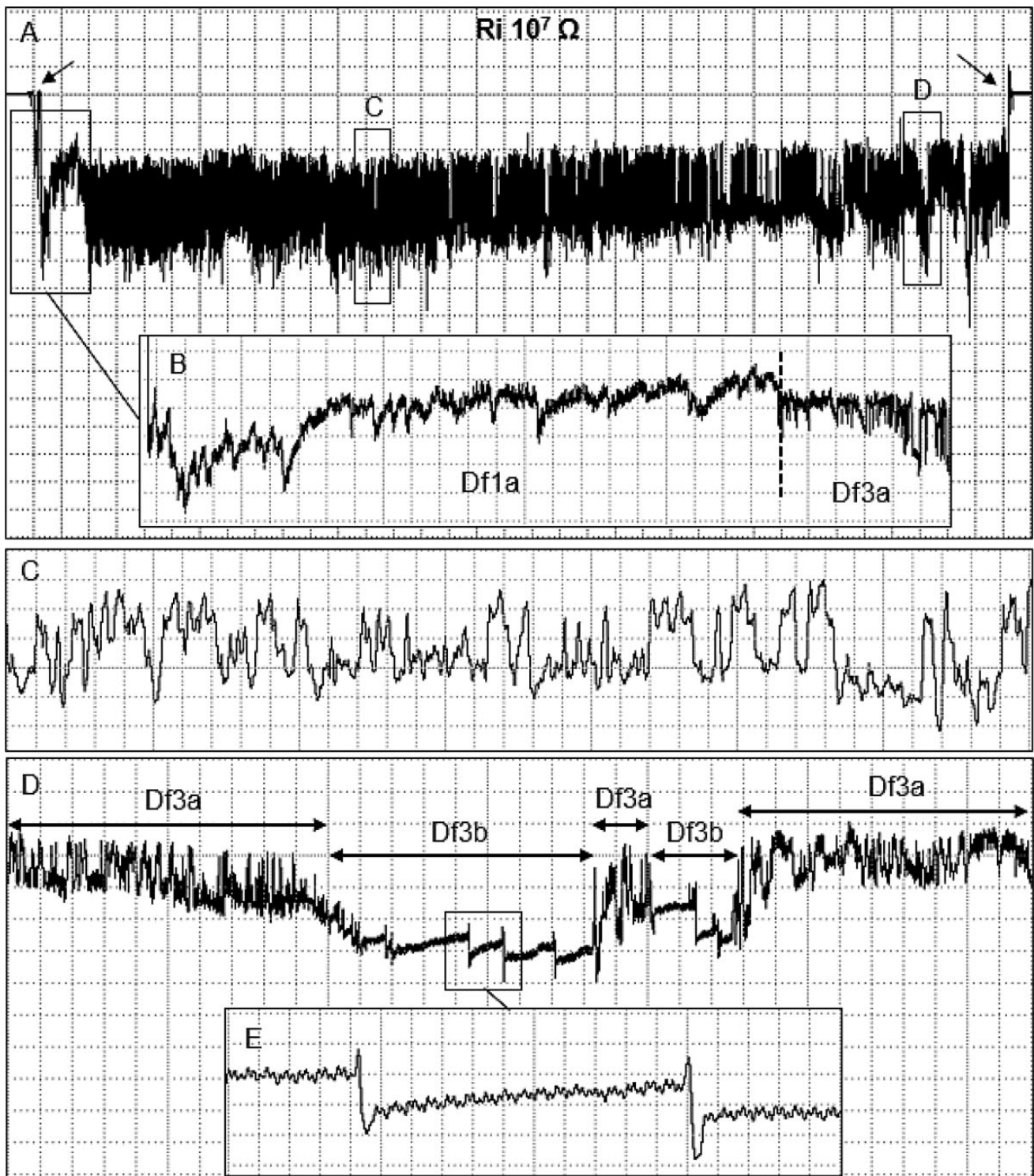


Fig. 3. Waveform Df3 recorded using EPG AC-DC from *Dichelops furcatus* on stems of wheat plants during vegetative stage (V3: tillering stage) at Ri 10^7 Ohms. (A) Compressed overview of a probing event (~60 min) showing waveforms Df1a (pathway) and Df3 (laceration/maceration activities and ingestion). (B) Expanded view of waveform Df1a and beginning of waveform Df3a. (C) Expanded view of waveform Df3a. (D) Details of the waveforms Df3a and Df3b. (E) Expanded view of waveform Df3b. (A has Windaq compression 500 [100 s/vertical div.], gain 16 \times ; B has compression 30 [6 s/vertical div.], gain 16 \times ; C has compression 3 [0.6 s/vertical div.], gain 16 \times ; D has compression 20 [4 s/vertical div.], gain 8 \times ; E has compression 2 [0.4 s/vertical div.], gain 16 \times). Arrowheads indicate beginning or end of a probe.

salivary sheath during Df1a. When this waveform was recorded before Df2 ($n=10$, stem), the salivary sheath was completely secreted (Fig. 7B), i.e., the full length of the stylets. However, when Df1a was recorded before Df3a on stem ($n=5$), or before Df4a on

seed endosperm ($n=2$), the salivary sheath was not completely formed (Fig. 7D–F).

Df2. Cuts made during the waveform Df2 on stem showed that in all histological sections ($n=10$), the tip of the salivary sheath

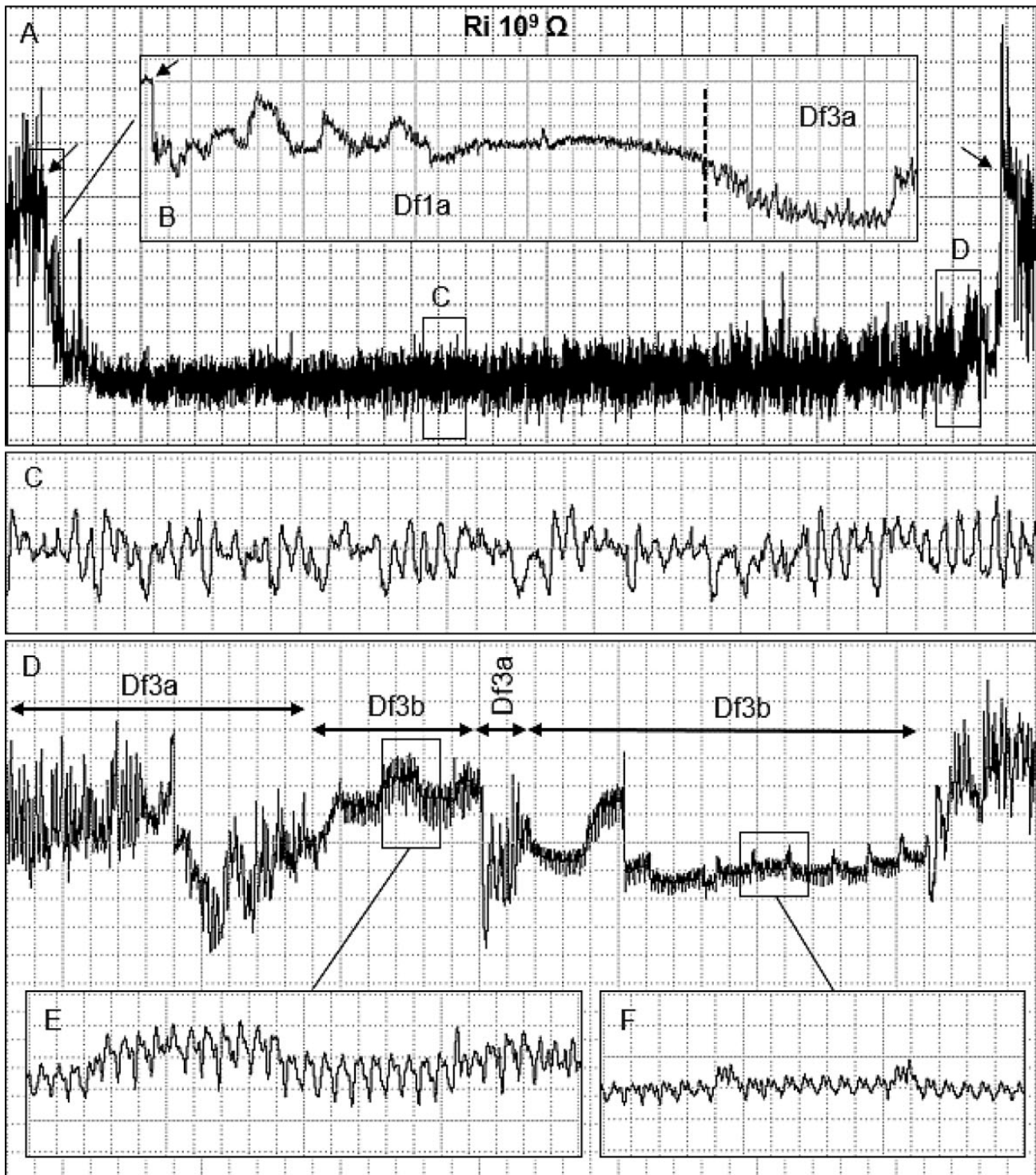


Fig. 4. Waveform Df3 recorded using EPG AC-DC from *Dichelops furcatus* on stems of wheat plants during vegetative stage (V3: tillering stage) at $Ri\ 10^9$ Ohms. (A) Compressed overview of a probing event (~50 min) showing waveforms Df1a (pathway) and Df3 (laceration/maceration activities and ingestion). (B) Expanded view of waveform Df1a and beginning of waveform Df3a. (C) Expanded view of waveform Df3a. (D) Details of the waveforms Df3a and Df3b. (E-F) Expanded views of waveform Df3b. (A has Windaq compression 400 [80 s/vertical div.], gain 16 \times ; B has compression 6 [1.2 s/vertical div.], gain 16 \times ; C has compression 3 [0.6 s/vertical div.], gain 32 \times ; D has compression 10 [2 s/vertical div.], gain 32 \times ; E and F have compression 2 [0.4 s/vertical div.], gain 32 \times). Arrowheads indicate beginning or end of a probe.

and/or stylets were positioned inside xylem cells (Fig. 7B). During Df2 in the wheat ear head, cuts made in the lemma layer ($n=2$) showed the stylets close to the xylem vessels (longitudinal position) in the plant tissue (Fig. 7C). However, the histological images did

not allow clarification of stylet tip positions, especially whether they were inside the xylem vessels or not.

Df3. During the Df3a wave (observed only in stems), the tip of the stylets ($n=5$) was always positioned in the parenchyma tissue

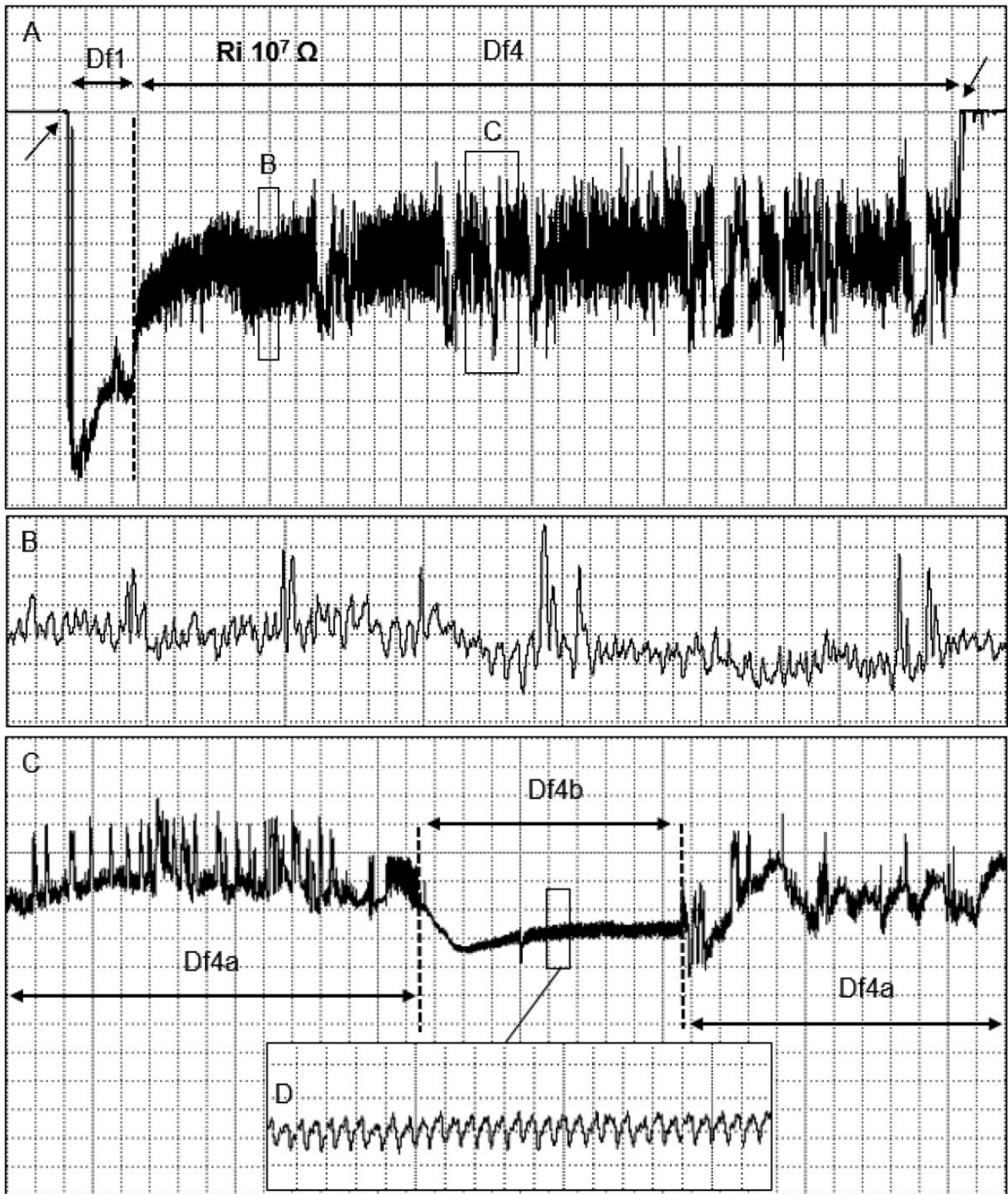


Fig. 5. Waveform Df4 recorded using EPG AC-DC from *D. furcatus* on ear head of wheat plants during reproductive stage (R11.1: milk grain stage) at $Ri\ 10^7$ Ohms. (A) Compressed overview of a probing event (~140 min) showing waveforms Df1 (pathway) and Df4 (laceration/maceration activities and ingestion). (B) Expanded view of waveform Df4a. (C) Details of the waveforms Df4a and Df4b. (D) Expanded view of waveform Df4b. (A has Windaq compression 1,200 [240 s/vertical div.], gain 8 \times ; B and D have compression 3 [0.6 s/vertical div.], gain 16 \times ; C has compression 30 [6 s/vertical div.], gain 8 \times). Arrowheads indicate beginning or end of a probe.

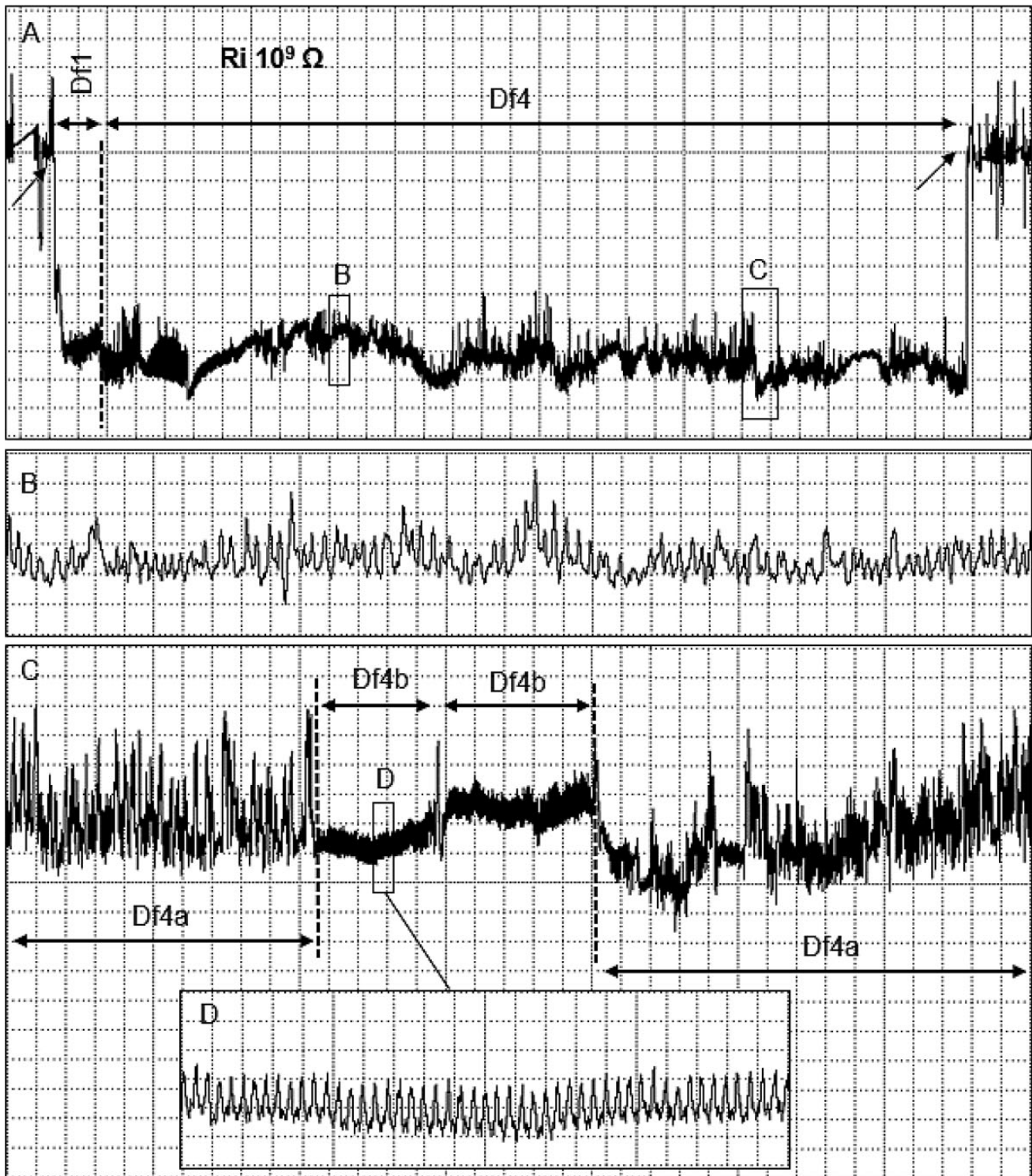


Fig. 6. Waveform Df4 recorded using EPG AC-DC from *D. furcatus* on ear head of wheat plants during reproductive stage (R11.1: milk grain stage) at Ri 10⁹ Ohms. (A) Compressed overview of a probing event (~60 min) showing waveforms Df1 (pathway) and Df4 (laceration/maceration activities and ingestion). (B) Expanded view of waveform Df4a. (C) Details of the waveforms Df4a and Df4b. (D) Expanded view of waveform Df4b. (A has Windaq compression 600 [120 s/vertical div.], gain 4×; B has compression 3 [0.6 s/vertical div.], gain 16×; C has compression 30 [6 s/vertical div.], gain 16×; D has compression 3 [0.6 s/vertical div.], gain 32×). Arrowheads indicate beginning or end of a probe.

(Fig. 7D) and there was also an incomplete secretion of the salivary sheath when this wave was recorded (Fig. 7E).

Df4. In the waveform Df4a (observed only in seed), the histological sections ($n=2$) showed the stylet tips positioned inside the seed

endosperm, and the formation of an incomplete salivary sheath (Fig. 7F, red arrow indicates the end of the salivary sheath).

Moreover, cuts made of fresh stems, after recording of a Df3 wave event ($n=6$), revealed a visibly damaged area (opaque region

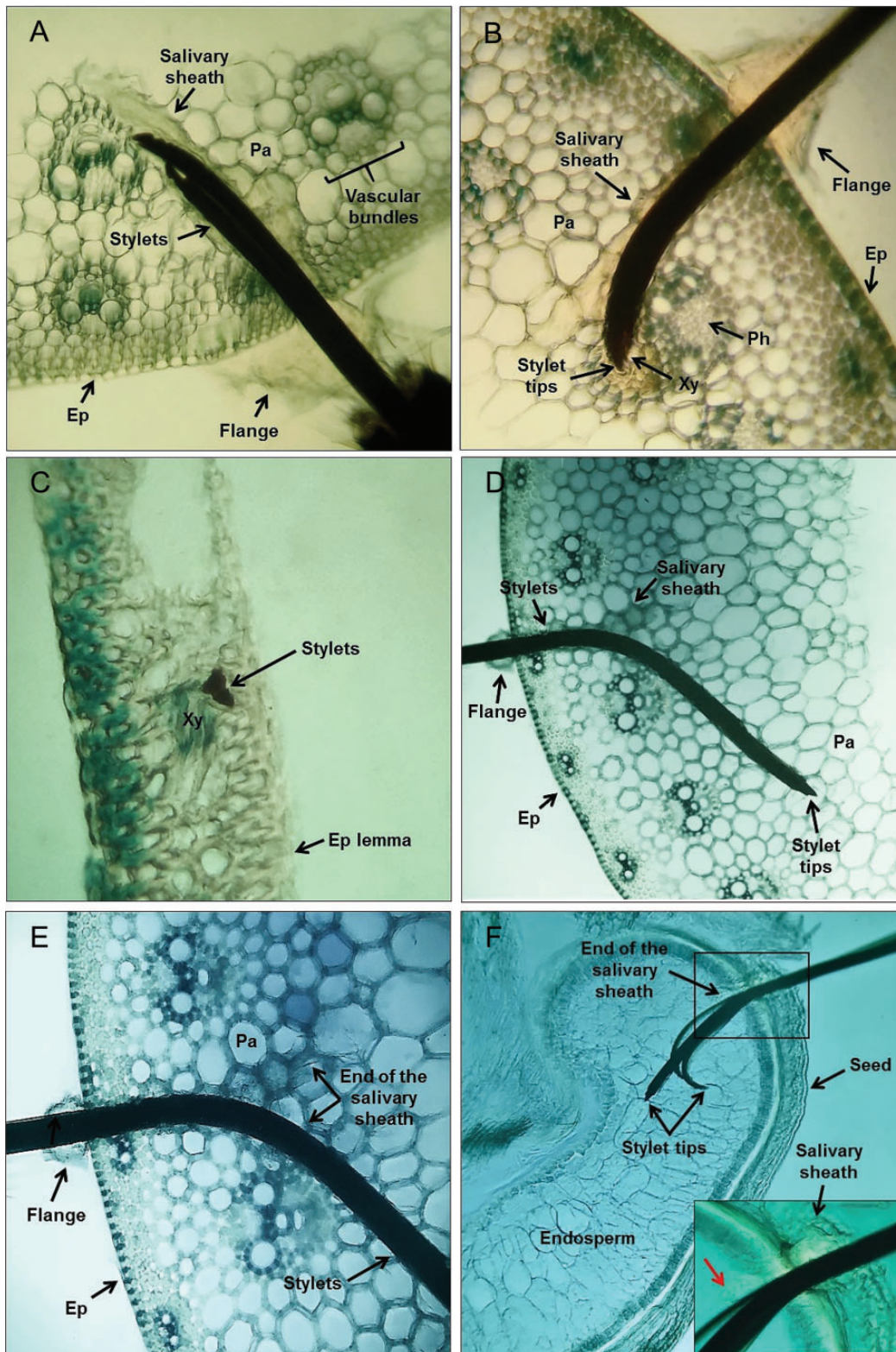


Fig. 7. Cross sections of wheat stems (V8 stage: flag leaf visible) and ear head structures (R11.1 stage: milk grain stage) containing severed stylets and salivary sheath of the stink bug *D. furcatus*. (A) Salivary sheath ending in the parenchyma tissue during waveform Df1a on stem. (B) Salivary sheath and stylet tips ending in the xylem vessels during waveform Df2 on stem. (C) Stylet tips near of xylem vessels during waveform Df2 on ear head (lemma layer). (D) Stylet tips in parenchyma tissue during waveform Df3a on stem. (E) Secretion of a flange (externally on the stem) and of an incomplete salivary sheath (internally in the tissue) during waveform Df3a on stem. (F) Stylet tips inside the seed endosperm during waveform Df4a and an incomplete salivary sheath secreted internally in the tissue (indicated by the red arrow in the detail box). Ep = stem epidermis, Ep lemma = lemma epidermis, Pa = parenchyma, Xy = xylem, Ph = phloem.

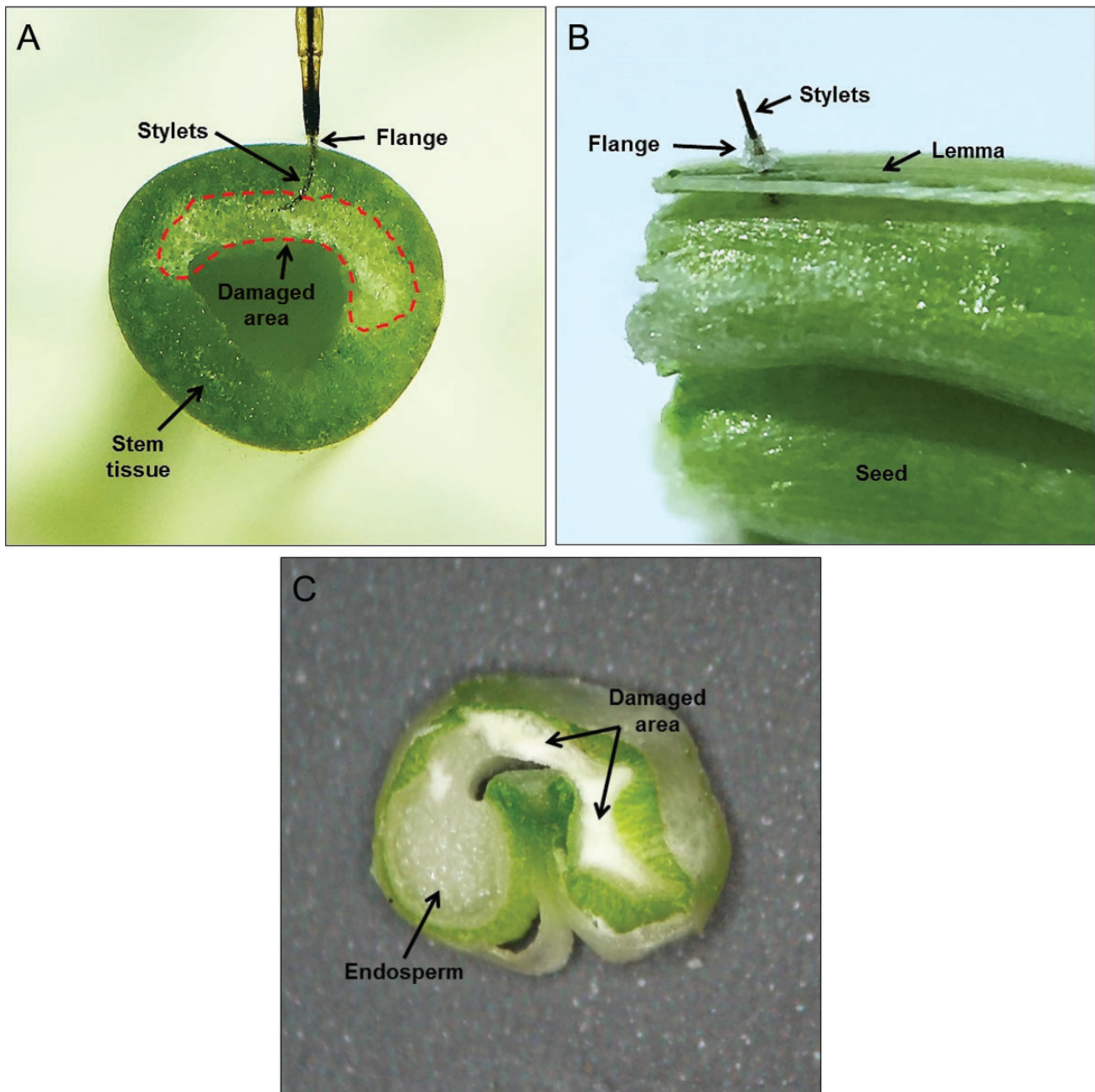


Fig. 8. Cross sections of fresh stem (V8 stage: flag leaf visible) and fresh seed (R11.1 stage: milk grain stage) of wheat plants containing cut stylets of *D. furcatus*. (A) Section of a fresh wheat stem showing damaged area (opaque region surrounded by the red line) after recording a Df3 wave event on stem. (B) Immature wheat seed containing the flange (externally on lemma layer) and cut stylets during waveform Df4 on seed. (C) Section of a fresh seed showing the damaged area (opaque region) after recording a Df4 wave event on seed endosperm.

surrounded by the red line, Fig. 8A). Similarly, cuts made in fresh seeds during the waveform Df4a ($n=8$) showed the stylets positioned in the seed endosperm, and the secretion of flanges externally on protection layers of the seed (Fig. 8B). In addition, cuts made in fresh seeds, after a Df4 wave event, showed a visually damaged area in the seed endosperm (region of opaque white color, Fig. 8C).

Discussion

In this study, the probing behavior of the pentatomid *D. furcatus*, found attacking the wheat crop in southern Brazil, was evaluated

using the AC-DC electropenetrography EPG technique. Seven different waveforms related to its probing behavior on stem (vegetative stage: V3) and ear head (reproductive stage: R11.1) of wheat plant were described.

Some similarities with other stink bugs already studied via EPG were observed during feeding of *D. furcatus* in both plant structures, as well as some interesting peculiarities. One of the most relevant similarities is the use of the same feeding strategy on stem and on ear head of wheat, in this case, the cell rupture feeding strategy [Backus et al. 2005–, previously known as laceration and flush strategy (Miles 1972)]. However, the waveforms recorded for each feeding site, even using the same strategy, were completely different in

appearance and electrical characteristics, which demonstrates the complexity of the *D. furcatus* feeding process. In addition, when the same bug ingests from xylem vessels, it uses another feeding strategy, known as salivary sheath strategy, which was demonstrated in the histological analyses.

Previous studies have shown that the same stink bug species may use only one of those strategies, such as *E. meditabunda* which uses the salivary sheath when feeding on soybean stems (Lucini and Panizzi 2016); or both strategies, as observed for *P. guildinii* on soybean plants (Lucini et al. 2016) and for *D. melacanthus* on maize seedlings (Lucini and Panizzi 2017). Similarly, when feeding on wheat plants *D. furcatus* also uses both feeding strategies, switching strategy according to the feeding site exploited.

Pathway phase is represented by a single waveform, Df1, which was divided into two subtypes, Df1a and Df1b. Df1a was the first waveform related to feeding of *D. furcatus* on the wheat plant, and was observed on both plant structures (stem and ear head), whereas Df1b was recorded only when bugs fed on wheat ear head. The subtype Df1a represents the insertion and deep penetration of the stylets into the plant tissue and also the secretion of gelling saliva to form the salivary sheath as observed in all the histological images from stems of wheat during this waveform. In addition, the secretion of salivary flanges (external deposition of gelling saliva) was frequently observed on stem and also on ear head of wheat. The subtype Df1b probably represents the bug encounter of a rigid cell layer requiring stylet protraction and retraction.

Similar to the present study, other EPG studies (Lucini and Panizzi 2016, 2017; Lucini et al. 2016) with other species of pentatomids showed that pathway phase was correlated, via histological studies, with salivary sheath secretion. It can be completely or incompletely formed, depending on the feeding strategy used by the bug. Complete secretion occurs when the bug uses the salivary sheath strategy to ingest from vessels of the vascular tissues: xylem and phloem (Bonani et al. 2010; Backus et al. 2013; Pearson et al. 2014; Lucini and Panizzi 2016, 2017; Lucini et al. 2016; Seo et al. 2016); incomplete secretion occurs during the cell rupture feeding strategy (Miles 1972, Backus et al. 2005).

Likewise, it was observed in the histological images of *D. furcatus* on wheat stem that during feeding activities in xylem vessels, the salivary sheath was completely formed and followed the pathway the stylets to the vessels. However, during the cell rupture activities on stem and on seed, a partial salivary sheath was observed to be formed. In the histological images of these plant structures during cell rupturing, a salivary sheath surrounding the stylet was observed only at the beginning of its insertion point in the plant tissue, similar to *D. melacanthus* on stem of maize seedlings (Lucini and Panizzi 2017).

We believe that Df1b represents the stylet work to overcome some physical barrier that makes the penetration of the stylets into the plant tissue quite difficult. The structures that make up the wheat spikelet are rigid and are the only layers responsible for protecting the seed.

A waveform very similar to Df1b, namely, Pg1d, was described for *P. guildinii* fed on different parts of the soybean pod. Pg1d was correlated with the bug forcing the stylets downward and subsequently retracting them upward. This indicates the presence of a rigid cell layer (which was observed in histological analyses of soybean pods) that was difficult to penetrate with the stylets, requiring stylet laceration to reach the seed (Lucini et al. 2016).

During the ingestion phase, one of the waveforms recorded was Df2, which was recorded when the bug fed on stem and on any structure of the ear head (palea, glume, lemma, or awn). Df2 was

correlated via histological analysis with activities in the xylem vessels, more specifically, sap ingestion. This wave was strongly similar in appearance to the Dm2 wave of *D. melacanthus* feeding on maize stem (Lucini and Panizzi 2017), which was also correlated to xylem sap activities. In addition, both waves (Df2 and Dm2) share some electrical characteristics, such as high-amplitude value at Ri 10⁹ Ohms, and a mixture of electrical origins for the peaks (R and emf) and waves (emf).

In fact, all *D. furcatus* bugs evaluated in both plant structures ingested from the xylem vessels. Probably this is a strategy to avoid dehydration and to maintain body water balance, as reported for other piercing-sucking insects such as aphids and psyllids (Spiller et al. 1990, Bonani et al. 2010, Pompon et al. 2010), and also for other species of stink bug (Lucini and Panizzi 2016). In case of ingestion of water during feeding on wheat seed, this may also be a strategy for nutrient dilution, since the seed is highly concentrated in nutrients (Panizzi and Slansky 1985), as observed for *P. guildinii* feeding on soybean seed endosperm (Lucini et al. 2016).

During ingestion phase using cell rupture feeding on stem (waveforms Df3a and Df3b), the bug (during the first subtype) makes rapid, continuous, and deep protraction and retraction of the stylets in the stem tissue. Such activity is reported in the literature to occur during the activities of laceration (mechanical action of stylets) and maceration (enzymatic action: digestive enzymes secreted in watery saliva) (Miles 1972, 1987), which are tactics of the cell rupture strategy (Backus et al. 2005). This behavior was also noted for other sucking insects, such as the leafhoppers *Empoasca fabae* (Harris), *Empoasca kraemeri* (Ross & Moore) (Calderon and Backus 1992), and *Empoasca vitis* Göthe (Jin et al. 2012), as well as stink bugs, *Lygus hesperus* Knight (Cline and Backus 2002), *P. guildinii* (Lucini et al. 2016), and *D. melacanthus* (Lucini and Panizzi 2017). In the last species, in one of the waveforms recorded on maize seedlings (called Dm3a), the bug moved its stylets in the stem tissue similar to that observed herein for the waveform Df3a of *D. furcatus* on wheat stem. Moreover, during Df3a, there was the secretion of an incomplete salivary sheath, as observed for *D. melacanthus* using the cell rupture strategy (Lucini and Panizzi 2017).

In the subtype Df3b, it was observed that the stylets remained motionless inside the plant tissue for a short period of time, and then, the stylets moved rapidly and vigorously in and out again (wave Df3a). Therefore, Df3b represents the ingestion of degraded cellular contents (composed of cells from parenchyma and possibly vascular vessels) via laceration and maceration activities, as described during the Dm3b wave of *D. melacanthus* (Lucini and Panizzi 2017). However, the waveform Df3b was not clearly distinguished and/or observed in all recordings in which the Df3a wave was recorded. Thus, we believe that during Df3a, the ingestion process may be occurring simultaneously with the laceration and maceration activities of the stem cells, as described for *D. melacanthus* during the Dm3a wave (Lucini and Panizzi 2017).

In addition to the similarities in the behavior of the two stink bugs *D. melacanthus* and *D. furcatus*, the subtypes Dm3a/Df3a and Dm3b/Df3b showed others similarities in appearance and in electrical characteristics. In the histological images made during the Df3a, it was not possible to observe a damaged area or cells destruction in the insertion region of the stylets. However, in fresh sections of the wheat stem was possible to clearly observe a damaged area of opaque white coloration.

During the ingestion phase using cell rupture feeding in the wheat ear head (seed endosperm: waveforms Df4a and Df4b), *D. furcatus* made a continuous and deep movement of the stylets in the wheat seed endosperm as reported during the waveform Pg3a

for *P. guildinii* feeding on soybean seed endosperm (Lucini et al. 2016). Therefore, the Df4a wave represents the dissolution of endosperm cells via laceration (mechanical action) and maceration (enzymatic action) for future ingestion. During this waveform, a salivary sheath was observed surrounding the stylets only at the beginning of the insertion point in the seed endosperm, i.e., the salivary sheath was incompletely secreted inside the tissue, which was observed in the histological sections.

In cuts made of fresh wheat seeds, shortly after the recording of the Df4 wave, we observed a damaged area in the seed endosperm caused by the activities of laceration, maceration and ingestion; this is similar to what was reported for *P. guildinii* during the waveform Pg3 recorded on soybean seed endosperm (Lucini et al. 2016).

During the subtype Df4b, the stylets of *D. furcatus* were motionless inside the seed tissue for a short period of time (which represents the ingestion period); after that, they moved their stylets again to break more cells (Df4a wave). This activity was continually repeated; however, the bug spent most of the time in laceration and maceration activities to prepare the food for latter ingestion, which usually took a short time.

In conclusion, our results demonstrated that *D. furcatus* feeding on wheat plants during vegetative (stem) and reproductive (ear head) stages use two different feeding strategies. When in xylem vessels (ingestion of xylem sap) on wheat stem (and probably on ear head although not histological demonstrated in this work), *D. furcatus* used the salivary sheath strategy, with its complete salivary sheath secretion. In contrast, when on seed endosperm and again on stem, the bug used the cell rupture strategy as well, using the laceration and maceration tactics to break cell pockets for ingesting. At this time, a salivary sheath was also observed in the plant tissue, however, not completely formed. These results demonstrate the plasticity of this insect's feeding behavior, which involve a switch in strategy according to the feeding site exploited.

Acknowledgments

This study was partially supported by a National Council of Research and Technology of Brazil grant 471517/2012-7 to A.R.P. and by a scholarship from CAPES (Ministry of Education) of Brazil to T.L. in order to obtain the Doctor of Science (Entomology) degree at the Federal University of Paraná at Curitiba, Brazil. We also thank the Embrapa Unit at Passo Fundo, RS, for support. Appreciation is also extended to Elaine Backus and Paula Mitchell for reviewing and earlier draft of the article. Approved by the Publication Committee of the Embrapa National Wheat Research Center, Passo Fundo, RS, Brazil, under number 5408/2016.

References Cited

- Ávila, C. J., and A. R. Panizzi. 1995. Occurrence and damage by *Dichelops (Neodichelops) melacanthus* (Dallas) (Heteroptera: Pentatomidae) on corn. *An. Soc. Entomol. Bras.* 24: 193–194.
- Backus, E. A., and W. H. Bennett. 2009. The AC-DC Correlation Monitor: New EPG design with flexible input resistors to detect both R and emf components for any piercing-sucking hemipteran. *J. Insect Physiol.* 55: 869–884.
- Backus, E. A., M. Rangasamy, M. Stamm, H. J. McAuslane, and R. Cherry. 2013. Waveform library for chinch bugs (Hemiptera: Heteroptera: Blissidae): characterization of electrical penetration graph waveforms at multiple input impedances. *Ann. Entomol. Soc. Am.* 106: 524–539.
- Backus, E. A., S. Serrano, and C. M. Ranger. 2005. Mechanisms of hopperburn: An overview of insect taxonomy, behavior, and physiology. *Annu. Rev. Entomol.* 50: 125–151.
- Bonani, J. P., A. Fereres, E. Garzo, M. P. Miranda, B. Appezzato-da-Gloria, and J. R. S. Lopes. 2010. Characterization of electrical penetration graphs of the Asian citrus psyllid, *Diaphorina citri*, in sweet orange seedlings. *Entomol. Exp. Appl.* 134: 35–49.
- Buntin, G. D., and J. K. Greene. 2004. Abundance and species composition of stink bugs (Heteroptera: Pentatomidae) in Georgia winter wheat. *J. Entomol. Sci.* 39: 287–290.
- Calderon, J. D., and E. A. Backus. 1992. Comparison of the probing behaviors of *Empoasca fabae* and *E. kraemeri* (Homoptera: Cicadellidae) on resistant and susceptible cultivars of common beans. *J. Econ. Entomol.* 85: 88–99.
- Chiaradia, L. A., A. Rebonatto, M. A. Smaniotto, M. R. F. Davila, and C. N. Nesi. 2011. Arthropods associated with soybean crops. *Rev. Ciênc. Agrovet.* 10: 29–36.
- Chocorosqui, V. R., and A. R. Panizzi. 2004. Impact of cultivation systems on *Dichelops melacanthus* (Dallas) (Heteroptera: Pentatomidae) populations and damage and its chemical control on wheat. *Neotrop. Entomol.* 33: 487–492.
- Cline, A. R., and E. A. Backus. 2002. Correlations among AC electronic monitoring waveforms, body postures, and stylet penetration behaviors of *Lygehavierrus* (Hemiptera: Miridae). *Environ. Entomol.* 31: 538–549.
- Ferreira, E., and P. M. Silveira. 1991. Dano de *Thyanta perditor* (Hemiptera: Pentatomidae) em trigo (*Triticum aestivum* L.). *An. Soc. Entomol. Bras.* 20: 165–171.
- Frota, R. T., and R. S. S. Santos. 2007. Pentatomidae bugs associated with sunflower crops in the northwest of Rio Grande do Sul state and the action of *Euschistus heros* (Fabricius, 1794) (Hemiptera: Pentatomidae) on sunflower seeds. *Biotemas.* 20: 65–71.
- Jin, S., Z. M. Chen, E. A. Backus, X. L. Sun, and B. Xiao. 2012. Characterization of EPG waveforms for the tea green leafhopper, *Empoasca vitis* Göthe (Hemiptera: Cicadellidae), on tea plants and their correlation with stylet activities. *J. Insect Physiol.* 58: 1235–1244.
- Koch, R. L., A. Rich, and T. Pahs. 2016. Statewide and season-long surveys for Pentatomidae (Hemiptera: Heteroptera) of Minnesota wheat. *Ann. Entomol. Soc. Am.* 109: 396–404.
- Large, E. C. 1954. Growth stages in cereals. Illustration of the Feekes scale. *Plant Pathol.* 3: 128–129.
- Lucini, T., and A. R. Panizzi. 2016. Waveform characterization of the soybean stem feeder *Edessa mediatubunda*: overcoming the challenge of wiring pentatomids for EPG. *Entomol. Exp. Appl.* 158: 118–132.
- Lucini, T., and A. R. Panizzi. 2017. Feeding behavior of the stink bug *Dichelops melacanthus* (Heteroptera: Pentatomidae) on maize seedlings: an EPG analysis at multiple input impedances and histology correlation. *Ann. Entomol. Soc. Am.* 110: *in press*. [Doi.org/10.1093/aesa/saw070](https://doi.org/10.1093/aesa/saw070).
- Lucini, T., A. R. Panizzi, and E. A. Backus. 2016. Characterization of an EPG waveform library for redbanded stink bug, *Piezodorus guildinii* (Hemiptera: Pentatomidae), on soybean plants. *Ann. Entomol. Soc. Am.* 109: 198–210.
- Miles, P. W. 1972. The saliva of Hemiptera. *Adv. Insect Physiol.* 9: 183–125.
- Miles, P. W. 1987. Plant-sucking bugs can remove the content of cells without mechanical damage. *Experientia.* 43: 937–939.
- Panizzi, A. R., and F. Slansky, Jr. 1985. Legume host impact on performance of adult *Piezodorus guildinii* (Westwood) (Hemiptera: Pentatomidae). *Environ. Entomol.* 14: 237–242.
- Panizzi, A. R., S. Corrêa, D. L. Gazzoni, E. B. Oliveira, G. G. Newman, and S. G. Turnipseed. 1977. Insects of soybean in Brazil. *Bol. Tec.*, n. 1. Embrapa, Londrina.
- Panizzi, A. R., T. Agostinetto, T. Lucini, and P. R. V. S. Pereira. 2016. Effect of green-belly stink bug, *Dichelops furcatus* (F.) on wheat yield and development. *Crop Prot.* 79: 20–25.
- Pearson, C. C., A. Backus, H. J. Shugart, and J. E. Munyaneza. 2014. Characterization and correlation of EPG waveforms of *Bactericera cockerelli* (Hemiptera: Trioziidae): Variability in waveform appearance in relation to applied signal. *Ann. Entomol. Soc. Am.* 107: 650–666.
- Pompon, J., D. Quiring, P. Giordanengo, and Y. Pelletier. 2010. Role of xylem consumption on osmoregulation in *Macrosiphum euphorbiae* (Thomas). *J. Insect Physiol.* 56: 610–615.
- Roza-Gomes, M. F., R. Salvadori, P. R. S. V. Pereira, and A. R. Panizzi. 2011. Injuries of four species of stink bugs to corn seedlings. *Cienc. Rural.* 41: 1115–1119.
- Seo, B. Y., K. Jung, C. G. Park, S. G. Lee, and Y. L. Park. 2016. Plant penetration activities by the flatid planthopper *Metcalfa pruinosa*

- (Hemiptera: Fulgoroidea): an electrical penetration graph-histology analysis. *J. Appl. Entomol.* 140: 706–714.
- Smaniotto, L. F., and A. R. Panizzi.** 2015. Interactions of selected species of stink bugs (Hemiptera: Heteroptera: Pentatomidae) from leguminous crops with plants in the neotropics. *Florida Entomol.* 98: 7–17.
- Spiller, N. J., L. Koenders, and W. F. Tjallingii.** 1990. Xylem ingestion by aphids – a strategy for maintaining water balance. *Entomol. Exp. Appl.* 55: 101–104.
- Tjallingii, W. F.** 1978. Electronic recording of penetration behaviour by aphids. *Entomol. Exp. Appl.* 24: 721–730.
- Walker, G. P.** 2000. A beginner's guide to electronic monitoring of homopteran probing behavior, pp. 14-40. *In* G. P. Walker and E. A. Backus (eds.), Principles and applications of electronic monitoring and other techniques in the study of homopteran feeding behavior. Thomas Say Publications in Entomology, Entomological Society of America, Lanham, MD.